Phosphoproteomics of Highly ABA-Induced1 identifies AT-Hook Like10 phosphorylation required for growth regulation during stress

Min May Wong[a,b,c], Govinal Badiger Bhaskara [a,1], Tuan-Nan Wen[a], Wen-Dar Lin[a], Thao Thi Nguyen[a,2], Geeng Loo Chong[a,b,c], Paul E. Verslues[a,b,d]

a. Institute of Plant and Microbial Biology, Academia Sinica, Taipei 115, Taiwan

b. Molecular and Biological Agricultural Sciences Program, Taiwan International Graduate Program, National Chung-Hsing University, Taichung 402, Taiwan and Academia Sinica, Taipei 115, Taiwan

c. Graduate Institute of Biotechnology, Biotechnology Center, National Chung-Hsing University, Taichung 402, Taiwan

d. Biotechnology Center, National Chung-Hsing University, Taichung 402, Taiwan

1. Present Address: Department of Integrative Biology, University of Texas, Austin, TX 78712

2. Present Address: Department of Biochemistry, University of Wisconsin, Madison, WI 53706

***Correspondence to:** Paul E. Verslues
Institute of Plant and Microbial Biology
Academia Sinica
No. 128 Sec. 2 Academia Rd, Nankang Dist.
Taipei, 11529
Taiwan
Phone: 886-2-2787-1186
FAX: 886-2-2782-7954
Email: paulv@gate.sinica.edu.tw

Short Title: HAI1 regulation of AHL10 identified by phosphoproteomics

Keywords: HAI1 protein phosphatase, phosphoproteomics, drought, AT-hook, AHL10

Abstract:

The Clade A protein phosphatase 2C Highly ABA-Induced 1 (HAI1) plays an important role in stress signaling yet little information is available on HAI1-regulated phosphoproteins. Quantitative phosphoproteomics identified phosphopeptides of increased abundance in *hai1-2* in unstressed plants and in plants exposed to low water potential (drought) stress. The identity and localization of the phosphoproteins as well as enrichment of specific phosphorylation motifs indicated that these phosphorylation sites may be regulated directly by HAI1 or by HAI1-regulated kinases including Mitogen-Activated Protein Kinases (MPKs), Sucrose-non fermenting Related Kinase 2 (SnRK2s) or Casein Kinases. One of the phosphosites putatively regulated by HAI1 was S313/S314 of AT Hook-Like10 (AHL10), a DNA binding protein of unclear function. HAI1 could directly dephosphorylate AHL10 *in vitro* and the level of *HAI1* expression affected the abundance of phosphorylated AHL10 *in vivo.* AHL10 S314 phosphorylation was critical for restriction of plant growth under low water potential stress and for regulation of Jasmonic Acid and Auxin-related gene expression as well as expression of developmental regulators including *Shootmeristemless* (*STM*). These genes were also mis-regulated in *hai1-2*. AHL10 S314 phosphorylation was required for AHL10 complexes to form foci within the nucleoplasm, suggesting that S314 phosphorylation may control AHL10 association with the nuclear matrix or with other transcriptional regulators. These data identify a set of HAI1-affected phosphorylation sites, show that HAI1-regulated phosphorylation of AHL10 S314 controls AHL10 function and localization and also indicate that HAI1-AHL10 signaling coordinates growth with stress and defense responses.

Introduction

Many types of environmental stress, both abiotic and biotic, limit plant growth. Drought stress is of particular interest and challenge because of its effect on crop productivity as well as our lack of understanding of the mechanisms plants use to sense and respond to soil drying and reduced water potential (ψ_w) during drought. Low ψ_w-induced accumulation of Abscisic Acid (ABA) controls downstream responses including growth and gene expression (1, 2). Plants perceive increased ABA levels via a pathway consisting of the PYR/PYL/RCAR ABA receptors (hereafter referred to as PYLs), Clade A protein phosphatase 2Cs (PP2Cs) and Sucrose Non-Fermenting Related Kinase 2 (SnRK2) protein kinases (3, 4). As ABA increases, formation of PYL-ABA-PP2C complexes inhibits PP2C activity. This releases suppression of SnRK2 activity by allowing the SnRK2s to autophosphorylate and phosphorylate downstream target proteins. Proteins regulated by SnRK2-mediated phosphorylation include nuclear and plasma membrane localized proteins. PYL-PP2C signaling can regulate Mitogen-activated Protein Kinase (MPK) signaling cascades which are active in ABA and abiotic stress signaling (5) in addition to their froles in defense signaling. Identification of phosphorylation sites regulated by SnRK2s, MPKs and ABA signaling is an area of active research (6-10). Despite the success of these studies in identifying kinase targets and stress-affected phosphorylation sites, phosphoproteomics has yet to be applied to identify regulatory targets of the Clade A PP2Cs. We are aware of only one phosphoproteomic study of plant PP2Cs, an analysis of Clade E PP2Cs (11).

Six of the nine Clade A PP2Cs were identified in forward genetic screens for altered ABA sensitivity of seed germination (see for example 12-14). Interestingly, the remaining three Clade A PP2Cs, Highly ABA-Induced1 (HAI1), AKT-Interacting Protein1 (AIP1)/HAI2, and HAI3, were not identified in such screens as their effect on ABA sensitivity of seed germination is less (15, 16). Gene expression of the *HAI* PP2Cs is strongly induced by ABA as well as drought and salt stress (15, 17). *HAI* PP2C mutants, and *hai1* in particular, had a strong effect on osmotic adjustment and maintenance of fresh weight at low ψ_w (15). The three HAI PP2Cs are not regulated by Enhancer of ABA co-Receptor 1 (EAR1), which promotes the activity of the six other Clade A PP2Cs and thereby affects ABA sensitivity (18). Also, Mine et al. (19) found that the HAI PP2Cs, but not the Clade A PP2C ABI2, could interact with MPK3 and MPK6. They also demonstrated that HAI1 could directly dephosphorylate these MPKs. *HAI1* was induced by coronatine-mediated activation of the JA-signaling factor MYC2 and HAI1 suppression of

MPK3 and MPK6 activation promoted virulence of *Pseudomonas syringae* (19). *HAI1* was also identified as a target of the transcription factor Scarecrow, a root development regulator (20). Together these studies indicate that there are both overlapping aspects and diversification among the Clade A PP2Cs in terms how strongly they affect specific stress and ABA-related phenotypes and how their phosphatase activity is regulated. The data also suggest a prominent role for HAI1 in coordination of abiotic stress, development, and defense responses

We used quantitative phosphoproteomics of *hai1-2* to identify phosphorylation sites putatively regulated by HAI1. One of the proteins with increased phosphopeptide abundance in *hai1-2* was AT-Hook Like10 (AHL10). Phosphorylation of AHL10 at the site affected by HAI1 was required for AHL10 to suppress growth, regulate expression of hormone and development related genes at low ψ_w and localize to foci within the nucleoplasm. These data indicate that HAI1 and AHL10 connect stress signaling to growth and developmental regulation.

Results

HAI1-affected phosphorylation sites identified by quantitative phosphoproteomics

Longer term low ψ_w stress strongly induces *HAI1* expression (15). Thus, quantitative phosphoproteomics of wild type and *hai1-2* was performed for seedlings maintained at high ψ_w (unstressed control) and for seedlings transferred to low ψ_w (-1.2 MPa) for 96 h. The analysis of *hai1-2* (Dataset S1) was conducted in the same set of iTRAQ labeling experiments as the wild type and Clade E Growth Regulating (EGR) PP2C data previously reported by our laboratory (11, 21). In the unstressed control, 61 phosphopeptides from 56 proteins were significantly more abundant in *hai1-2* compared to wild type while only 18 phosphopeptides from 17 proteins were significantly less abundant (Dataset S2). Similarly, at low ψ_w 40 phosphopeptides from 39 proteins were significantly more abundant in *hai1-2* while 8 phosphopeptides from 7 proteins were less abundant (Dataset S3). Even proteins with highly increased phosphopeptide abundance had no significant change in gene expression in *hai1-2* (Fig. 1A, the *hai1-2* transcriptome data has been discussed previously (15)). Thus, phosphoproteomics identified a different set of HAI1-affected loci than transcriptome analysis. Four proteins had increased phosphopeptide abundance in both control and stress treatments (SI Appendix Fig. S1). While this limited overlap could

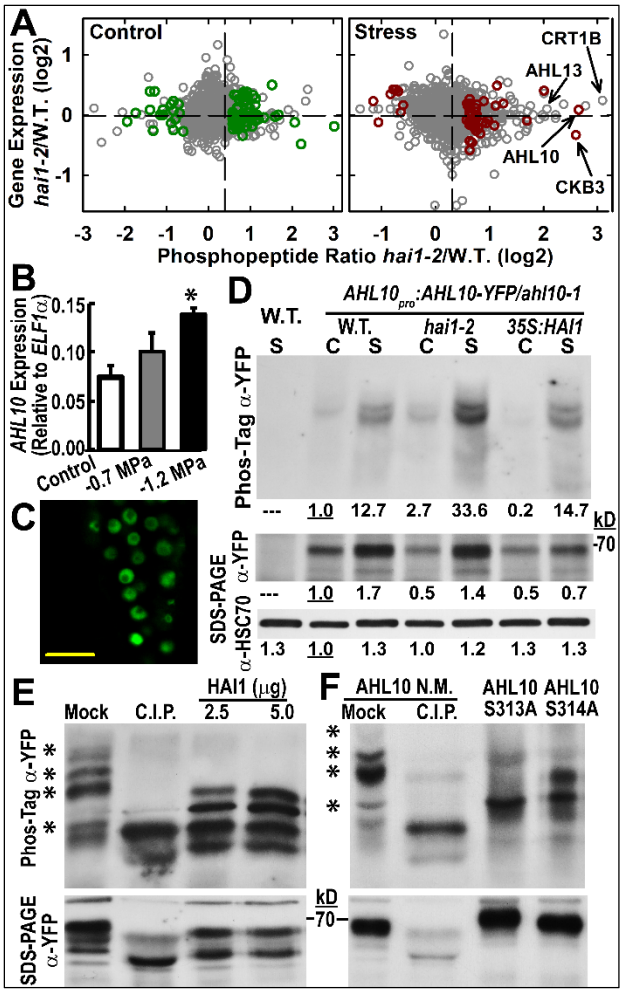

Figure 1: Phosphoproteomics of *hai1-2* identifies a set of HAI1-affected phosphoproteins, including AHL10 which is a HAI1 dephosphorylation substrate.

A. Phosphopeptide abundance versus gene expression for *hai1-2* compared to wild type. Dark green or red symbols indicate phosphopeptides with significantly increased or decreased abundance (P ≤0.05 by one sided T-test and fold change ≥ 1.5) in *hai1-2* compared to wild type for control and stress (-1.2 MPa, 96 h) treatments (Dataset S2, S3). Other phosphopeptide data are plotted using gray symbols (Dataset S1). Transcriptome analysis of *hai1-2* has been previously described (15).
B. *AHL10* gene expression in wild type for unstressed control or 96 h after transfer to two different severities of low ψ_w stress (-0.7 and -1.2 MPa). Data are means ± SE, n = 3. Asterisk (*) indicates significant difference compared to control (P ≤0.05 by T-test).
C. AHL10 localization in plants expressing *AHL10$_{promoter}$:AHL10-YFP* in the *ahl10-1* mutant background. Cells in root tip of unstressed seedlings are shown. An essentially identical localization pattern was observed in stress treated seedlings. Scale bar = 20 μm.

D. Effect of HAI1 on *in vivo* phosphorylation status of AHL10 analyzed by introducing *AHL10$_{promoter}$:AHL10-YFP/ahl10-1* into *hai1-2* and *35S:FLAG-HAI1* backgrounds. Aliquots of the same samples were run on Phos-Tag (top) and SDS-PAGE (middle) gels and band intensities of AHL10-YFP quantified (25 μg protein loaded per lane for both gels). The SDS-PAGE blot was stripped and re-probed to detect HSC70 as a loading control. "C" indicates samples from the unstressed control while "S" indicates stress treatment (-1.2 MPa, 96 h). Note that unphosphorylated AHL10 could not be resolved on these Phos-Tag gels because long run time was used to better resolve highly phosphorylated AHL10. The experiment was repeated with consistent results.
E. AHL10-YFP immunoprecipitated from *AHL10$_{promoter}$:AHL10-YFP/ahl10-1hai1-2* plants after exposure to -1.2 MPa stress was dephosphorylated using recombinant HAI1 or Calf Intestinal Phosphatase (C.I.P.). Aliquots of the same samples were run on Phos-tag gel or SDS-PAGE. Asterisks (*) along the Phos-Tag blot indicate phosphorylated forms of AHL10 which were dephosphorylated (shifted down in the Phos-Tag gel) by C.I.P. treatment. The experiment was repeated with consistent results.
F. Phos-Tag gel analysis of non-mutated (N.M.) and phosphonull AHL10 (S313A, S314A) immunoprecipitated from plants expressing *35S:YFP-AHL10* in the *ahl10-1* mutant background. Experimental conditions were the same as for E and asterisks mark bands of phoshorylated AHL10 present in the N.M. lane.

indicate that HAI1 regulates different sets of proteins in the control and stress conditions, the incomplete coverage of the phosphoproteome should also be kept in mind.

The *hai1-2* affected phosphorylation sites were enriched in several specific phosphorylation motifs (SI Appendix Fig. S2; Dataset S4). These included the [pSP] motif, consistent with phosphorylation by MPKs and other proline-directed kinases (10) as well as variations of the [RxxpS] motif which can be targeted by SnRKs and Calcium Dependent Protein Kinases (CPKs) (22) and serine surrounded by acidic residues (E or D) which may be recognized by Casein kinase II (23). Consistent with these enriched motifs, five of the putative HAI1 target proteins are also putative SnRK2 substrates (Dataset S5) (6, 7, 24). Also consistent with enrichment of the [RxxpS] motif, a phosphopeptide from CPK9 was more abundant in *hai1-2* (Dataset S2), suggesting that HAI1 may affect some [RxxpS] sites via regulation of CPKs as well as SnRK2s. Similarly, the proteins with phosphopeptides increased in *hai1-2* included three known MPK substrates, Phos32 (25), SCL30 (26) and AT1G80180 (10), as well as 12 putative MPK substrates (Dataset S5) (9, 27). In relation to Casein kinases, a phosphopeptide from Casein Kinase 2 Beta Chain3 (CKB3) was increased in *hai1-2* under stress (Figure 1A) and a phosphopeptide from Casein Kinase1-Like Protein2 (CKL2) was increased in *hai1-2* in the control (Dataset S2). This was consistent with the enrichment of casein kinase phosphorylation motifs and observations that CKL2 affects ABA response (28, 29).

The proteins with increased phosphopeptide abundance in *hai1-2* under stress had a high prevalence of nuclear and plasma membrane localized proteins (SI Appendix Fig. S3). This was consistent with predominant localization of HAI1 in the nucleus but also partially along the plasma membrane (15, 30). Several of the proteins with increased phosphopeptide abundance in *hai1-2* have been previously found to be ABA or stress regulated. These include AKS1, AtSIK1, Annexin1 and the phosphatidic acid binding protein PLDRP1 (31). Interestingly several mRNA splicing-related proteins (RSP31, SCL30, RSZp22, RSZp33) were affected by *hai1-2* (Dataset S2, S3), consistent with previous reports that splicing protein phosphorylation is altered by stress or ABA and may be regulated by SnRK2 kinases (6, 7). It should be noted that our 96 h stress treatment (96 h), was advantageous to allow induction of *HAI1* expression. However, because of this longer stress treatment changes in phosphopeptide abundance could be influenced by changes in protein abundance as well as change in phosphorylation stoichiometry. While keeping

this caveat in mind, the *hai1-2* phosphoproteomics dataset is overall a useful resource to uncover signaling mechanisms influenced by HAI1.

AT-Hook Like10 (AHL10) interacts with and is dephosphorylated by HAI1

Bimolecular flourescence complementation (BiFC) assays were used as an initial screen for proteins which could be directly targeted by HAI1 (SI Appendix Fig. S4A). HAI1 interacted with AHL10 and CKB3, which had large increases in phosphopeptide abundance in *hai1-2* at low ψ_w (Fig. 1A), as well as a bZIP transcription factor (AT2G31370) which had a putative, but not significant, increase in phosphopeptide abundance (Dataset S1). Conversely, we did not see interaction with Calreticulin 1B (CRT1B, AT1G09210), which had the largest fold increase of all phosphopeptides but was variable and not significant (Fig. 1A), or PHOS32 and NF-YC11 (SI Appendix Fig. S4A).

We focused further attention on AHL10. Phosphopeptides with either AHL10 S313 or S314 phosphorylation were identified (SI Appendix Fig. S5). The AHL10 S313 phosphopeptide was strongly increased in *hai1-2* under stress (Fig. 1A, Dataset S3) while *AHL10* gene expression was only slightly increased by stress in wild type (Fig. 1B) and not affected by *hai1-2* (Fig. 1A). Note that there was some ambiguity in assigning the phosphorylation site to S313 or S314 in both of the AHL10 phosphopeptides identified. The same peptide with putative S313/S314 phosphorylation was identified previously (6, 7, 26). Interestingly, a phosphopeptide from AHL13 (AT4G17950) was also putatively (but not significantly) increased in *hai1-2* at low ψ_w (Fig. 1A, Dataset S1, SI Appendix Fig. S6). AHL10 and AHL13 are closely related Clade B AHLs (SI Appendix Fig. S7A) and the AHL10 S314 and AHL13 phosphorylation sites are in equivalent positions in the C-terminal region of both proteins (SI Appendix Fig. S7B). Other Clade B AHLs lacked this phosphorylation site.

Ratiometric BiFC (rBiFC) comparison of relative interaction intensity found that HAI1-AHL10 interaction was promoted by low ψ_w (SI Appendix Fig. S4B, C). AHL10 also interacted with HAI2 and HAI3. The HAI PP2C-AHL10 interaction occurred in a diffuse pattern in the nucleoplasm. A similar diffuse localization in the nucleoplasm and exclusion from the nucleolus was seen in transgenic plants expressing $AHL10_{promoter}$:*AHL10-YFP* in the *ahl10-1* background (Fig. 1C).

Phos-tag gel analysis found that in plants with wild type level of HAI1, phosphorylated AHL10 (seen as two bands on Phos-Tag gel) increased approximately 10-fold under low ψ_w stress compared to control (Fig. 1D) while AHL10 total protein increased only 1.7-fold (Fig. 1D, SDS-PAGE). This was similar to the increase in *AHL10* gene expression (Fig. 1B). There was further increase of phosphorylated AHL10 in *hai1-2* (Fig. 1D). Conversely, HAI1 ectopic expression (*35S:HAI1*) caused the amount of phosphorylated AHL10 to decrease in the control but had no additional effect during stress, presumably because endogenous HAI1 was already highly expressed. These results indicated that HAI1 restricted the level of phosphorylated AHL10. Despite the action of HAI1, abundance of phosphorylated AHL10 increased during low ψ_w stress. This was partially because of increased AHL10 protein level and also likely because of increased kinase activity to phosphorylate AHL10. Note that in Phos-Tag gel analysis of total protein extracts we were unable to resolve non-phosphorylated AHL10.

To test whether HAI1 could directly dephosphorylate AHL10, AHL10-YFP was immunoprecipitated from *AHL10*$_{promoter}$*:AHL10-YFP/ahl10-1hai1-2* plants and analyzed on Phos-Tag gels after *in vitro* phosphatase treatment. In mock incubated samples (no phosphatase), multiple bands of phosphorylated AHL10 could be observed (Fig. 1E), consistent with PhosPhAt listing of three experimentally observed AHL10 phosphosphorylation sites in addition to S313 and S314. Incubation with non-specific phosphatase (C.I.P.) completely dephosphorylated AHL10 (Fig. 1E). Treatment with recombinant HAI1 eliminated the most highly phosphorylated AHL10 bands (those having slowest migration on Phos-Tag gel) but did not completely dephosphorylate AHL10. Immunoprecipitation of AHL10 S313A and S314A phosphonull proteins showed that the same bands of phosphorylated AHL10 that were removed by HAI1 were also absent or shifted down in AHL10 S313A and S314A (Fig. 1F). These data indicated that HAI1 could directly dephosphorylate AHL10 S313 and S314.

AHL10 phosphorylation at S314 is critical for suppression of growth during moderate severity low ψ_w stress.

The effect of HAI1 on AHL10 phosphorylation suggested that AHL10 may also be involved in low ψ_w response. Consistent with this *ahl10-1* (SI Appendix Fig. S8A), had nearly forty percent higher rosette weight than wild type after an extended period of moderate severity soil drying (Fig. 2A, B). A similar enhanced growth maintenance of *ahl10-1* was seen in plate-

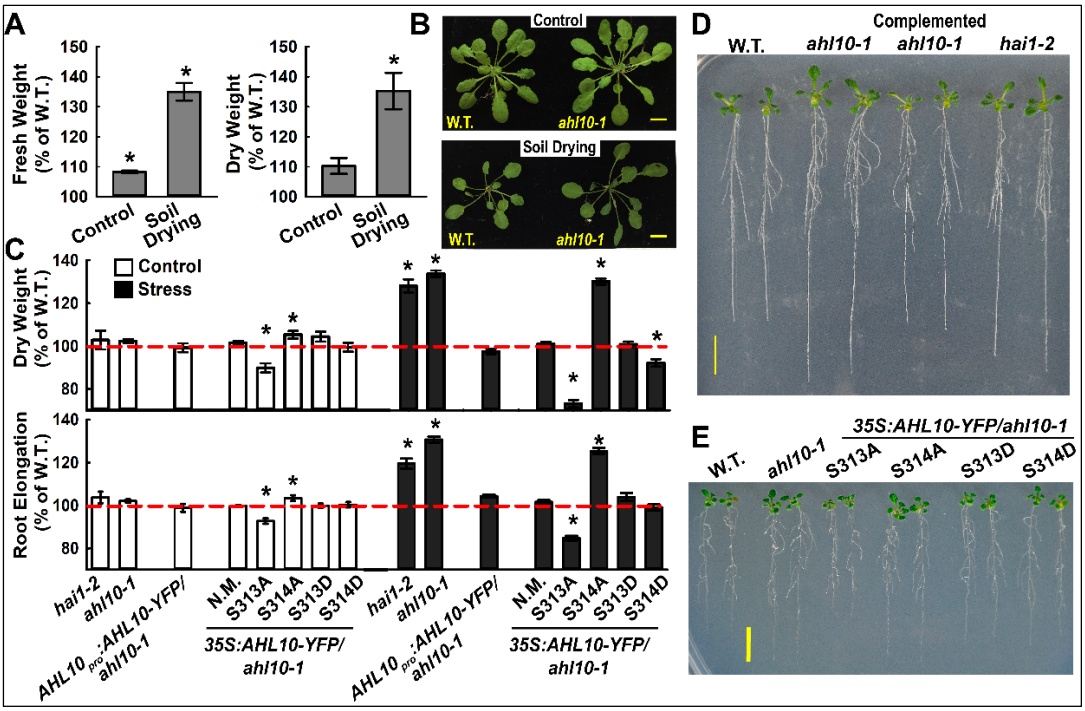

Figure 2: AHL10 phosphorylation at S314 is critical for growth suppression during moderate severity low ψ_w stress.

A. Relative Rosette fresh weight and dry weight of *ahl10-1* compared to Col-0 wild type in control or soil drying treatments (mean ± SE, n = 14-16 * indicates P ≤ 0.05 by one-sided t test).
B. Representative rosettes of the wild type and *ahl10-1* in control and soil drying treatments. Scale bars = 1 cm.
C. Root elongation and dry weight of seedlings under control and stress (-0.7 MPa) conditions. Data are relative to the Col-0 wild type (mean ± SE, n = 30 to 45, combined from three independent experiments). Asterisk (*) indicates significant difference compared with the wild type by one-sided test (P ≤ 0.05). Dashed red line indicates the wild type level (100%). Representative seedling weights and root elongation of Col-0 wild type used for normalization are shown in SI Appendix Fig S7. Note that three independent transgenic lines were analyzed for each construct and combined data of all three is shown. For the *35S:YFP-AHL10/ahl10*, N.M. indicates Non Mutated (ie: wild type) AHL10.
D. Representative seedlings of Col-0 wild type (W.T.), *ahl10-1*, *AHL10$_{promoter}$:AHL10-YFP/ahl10-1* (Complemented *ahl10-1*) and *hai1-2.* Five-day-old seedlings were transferred to -0.7 MPa and pictures taken 10 days after transfer when the quantitation of root elongation and seedling weight was performed. Scale bar = 1 cm.
E. Representative seedlings of Col-0 wild type (W.T.) and *ahl10-1* complemented with wild type AHL10 (N.M. = Not Mutated), phosphonull AHL10 (S313A, S314A) or phosphomimic AHL10 (S313D, S314D) all expressed under control of the *35S* promoter (*35S:YFP-AHL10*). Five-day-old seedlings were transferred to -0.7 MPa and pictures taken 10 days after transfer when the quantitation of root elongation and seedling weight was performed. Scale bar = 1 cm.

based assays where seedlings were transferred to moderate severity -0.7 MPa low ψ_w (Fig. 2C, D; wild type root length and dry weights as well as fresh weight of all genotypes at the time of transfer are shown in SI Appendix Fig. S9). The increased seedling weight and root elongation of *ahl10-1* could be complemented by *AHL10*$_{promoter}$*:AHL10-YFP* and *35S:YFP*-AHL10 (Fig. 2 C, D; *35S:YFP-AHL10* is labeled "N.M." for Not Mutated). *hai1-2* also had increased seedling weight and root elongation at low ψ_w.

To test the functional importance of AHL10 phosphorylation, phosphonull (S313A or S314A) and phosphomimic (S313D or S314D) AHL10 were expressed in the *ahl10-1* background. AHL10^{S314A} was unable to complement *ahl10-1* while AHL10^{S314D} and AHL10^{S313D} did complement (Fig. 2C, E). AHL10^{S313A} suppressed growth below the wild type level in both control and stress treatments. These data show that AHL10 function in growth regulation is dependent on S314 phosphorylation. The greater suppression of growth in AHL10^{S313A} indicates that S313 may act as a "decoy" site such that either S313 or S314 can be phosphorylated by the kinase(s) acting on AHL10. When S313 phosphorylation is blocked more S314 phosphorylation occurs leading to increased AHL10 function in growth suppression. However, other mechanisms cannot be ruled out. Note that three independent transgenic lines were used for each AHL10 construct and had indistinguishable growth phenotypes despite some difference in AHL10 protein level (SI Appendix Fig. 8B). Thus, the combined data of all three lines for each construct is shown in Fig. 2A. All of the AHL10 phosphomimic and null proteins were localized in the nucleus; however, we noted that localization of AHL10^{S313D} and AHL10^{S314D} was less diffuse and partially clustered into foci (SI Appendix Fig. S8C).

AHL10 regulates the expression of developmental and hormone-associated genes during drought acclimation.

To learn how AHL10 could influence growth, RNAseq was conducted for wild type and *ahl10-1* under unstressed conditions or moderate severity low ψ_w stress (-0.7 MPa, 96 h) where the growth maintenance phenotype of *ahl10-1* was apparent. In wild type 2212 genes were up-regulated and 2766 down regulated at low ψ_w (Dataset S6, S7; fold change in expression >1.25, adjusted $P \leq 0.05$). *HAI1* was strongly upregulated by low ψ_w (Dataset S6) in agreement with previous data (15). In *ahl10-1* there was little effect on gene expression in the unstressed control as only 10 genes had higher expression and 7 genes (excluding *AHL10* itself) had reduced

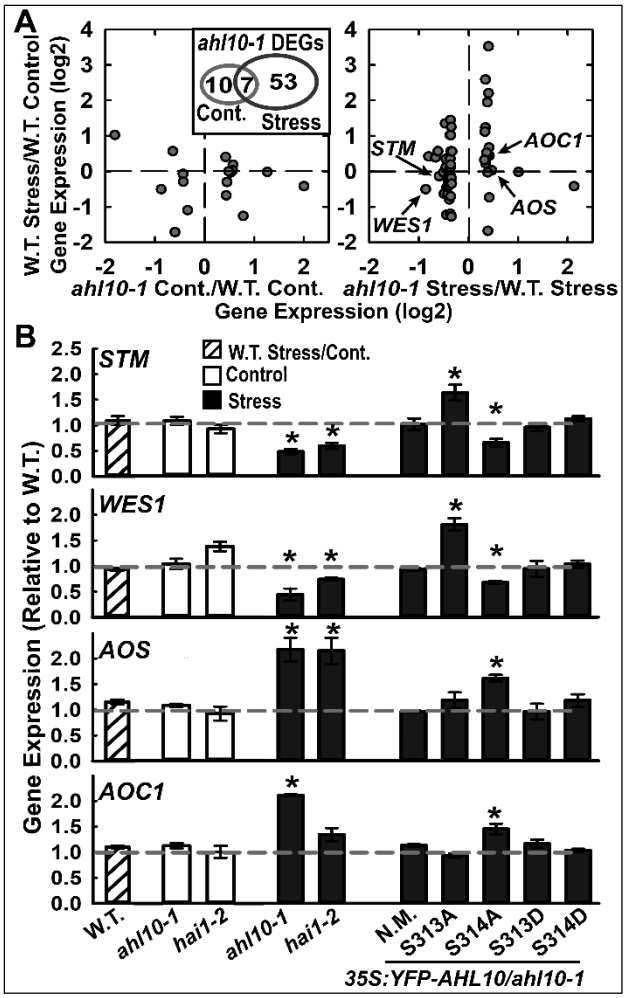

Figure 3: AHL10 regulation of development and hormone-related genes during low ψ_w stress also depends upon S314 phosphorylation.

A. Differentially expressed genes (DEGs) in *ahl10-1* discovered by RNAseq. Genes with differential expression in *ahl10-1* under either control or stress (-0.7 MPa, 96 h) plotted versus their expression in wild type stress versus wild type control. Inset shows the overlap between genes with differential expression in *ahl10-1* in control or stress treatments.

B. QPCR assay of selected genes in wild type stress (-0.7 MPa, 96 h) versus control as well as *ahl10-1*, *hai1-2* and AHL10 phosphomimic and null complementation lines. Data are shown as expression relative to wild type and are means ± SE, (n = 3) combined from three independent experiments. Asterisk (*) indicates significant difference compared to wild type in the same treatment (or wild type stress versus control) by one-sided test ($P \leq 0.05$). Gray dashed line indicates the wild type level (set to 1).

expression compared to wild type (Dataset S8). There was more effect of *ahl10-1* at low ψ_w where 19 genes were increased and 41 genes decreased compared to wild type (Dataset S9). The majority of genes differentially expressed in *ahl10-1* under stress were also differentially expressed in wild type at low ψ_w compared to the unstressed control. However, there was no concordance between the effect of stress in wild type (increased or decreased expression) and the direction of the *ahl10-1* effect (Fig. 3A). Only seven genes were differentially expressed in *ahl10-1* in both control and low ψ_w treatments (Fig. 3A, inset). Six of these were transposons or "other RNA" rather than protein coding genes.

The genes differentially expressed in *ahl10-1* at low ψ_w were consistent with altered growth regulation. These included *Shootmeristemless* (*STM*), a transcription factor required for meristem maintenance (32, 33) and two auxin-amido synthase genes (*WES1* and *DFL1*) that affect growth by controlling the level of active auxin (34-36). *WES1* is also known to be regulated by stress and ABA (34). Genes with increased expression in *ahl10-1* at low ψ_w included *Root Meristem Growth Factor 9* (*RGF9*), which is one of a family of genes that affect proliferation of transient amplifying cells in the root meristem (37), as well as the JA synthesis genes *Allene Oxide Synthase* (*AOS*) and *Allene Oxide Cyclase* (*AOC1*) and JA-responsive genes *JR2* and *VSP2* (38, 39). Many of these genes, for example *STM* and *RGF9*, have tissue specific expression. Thus their change in expression in meristems or other specific tissues may be more dramatic more than that seen in the whole seedling data shown here.

Quantitative RT-PCR validated that *STM* and *WES1* (Fig. 3B) as well as other genes (SI Appendix Fig. S10A) had decreased expression in *ahl10-1* at low ψ_w. Similarly, *AOS*, *AOC1* (Fig. 3B) and other genes (SI Appendix Fig. S10B) were confirmed to have increased expression in *ahl10-1* at low ψ_w. Consistent with the growth assays, AHL10^{S314A} was unable to complement the altered gene expression of *ahl10-1* while non-mutated (N.M.) AHL10 and AHL10^{S314D} could complement (Fig. 3B). For *STM* and *WES1* we again observed that AHL10^{S313A} acted as a hyper-functional allele having the opposite effect as *ahl10-1* (Fig. 3B). Also consistent with the growth assays, *hai1-2* had similar effect on gene expression at low ψ_w as *ahl10-1* (Fig. 3B).

AHL10 S314 phosphorylation does not affect AHL10 self-interaction but is required for AHL10 complexes to form nuclear foci.

The above results raised the question of how phosphorylation affects AHL10 protein function. Structural modeling confirmed that AHL10 S314 is in a loop region not immediately adjacent to the two AT-hook DNA binding domains or the PPC/DUF296 domain involved in AHL trimer formation (SI Appendix Fig. S11). This variable C-terminal portion of AHLs is thought to be involved in interaction of AHL complexes with other transcriptional regulators (40). AHL10 S313 and S314 phosphomimic and phosphonull variants had no effect on self-interaction in rBiFC assays (Fig. 4A, rBiFC images are in SI Appendix Fig. S12). Strikingly, for non-mutated AHL10 (N.M.), phosphomimic (S313D, S314D) and AHL10^{S313A}, the rBiFC flourescence from AHL10 complexes could often be seen as foci within the nucleus (Fig. 4B, C). The portion of nuclei with AHL10 foci increased under stress and was dramatically increased by the S313A mutation (Fig. 4C). In contrast, AHL10^{S314A} did not form foci and remained dispersed in the nucleoplasm (Fig. 4B, C). These data, along with reports that AT-hook proteins can associate with the nuclear matrix (41, 42), raise the possibility that interaction with the nuclear matrix or recruitment of AHL10 complexes to matrix attachment regions is dependent upon S314 phosphorylation.

Discussion

We identified a diverse set of proteins with altered phosphopeptide abundance in *hai1-2* compared to wild type. Given the strong effect of HAI1 on drought-related phenotypes, it is likely that many of these HAI1-affected phosphoproteins have previously unknown roles in drought response. The phosphorylation sites we identified likely represent a combination of sites directly dephosphorylated by HAI1 and sites phosphorylated by HAI1-regulated kinases (or both). AHL10 is a good example as the S314 phosphorylation site contained a Ser-Pro phosphorylation motif that is typically targeted by MPKs and the analogous phosphoserine site on AHL13 was identified as a putative MPK target (19). Thus, even though HAI1 could dephosphorylate AHL10 *in vitro*, AHL10 phosphorylation *in vivo* may also be affected by HAI1 dephosphorylation of MPKs (or other kinases) as well as activation of MPK activity by environmental stimuli (see model in SI Appendix Fig. S13). Consistent with this idea, the level of phosphorylated AHL10 increased in *hai1-2* in the unstressed control even though AHL10 and

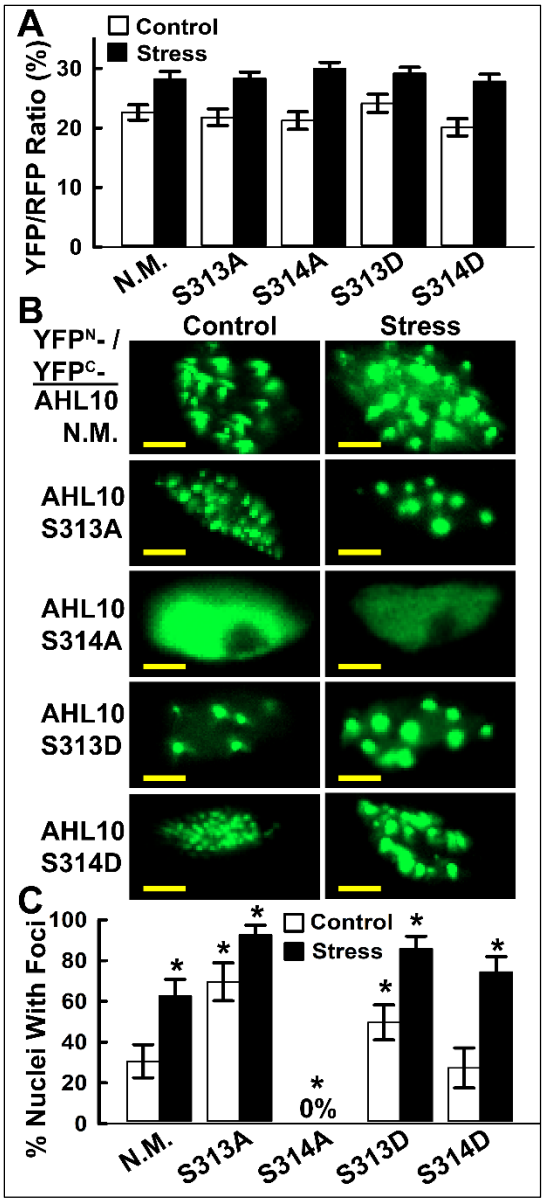

Figure 4: Ratiometric BiFC (rBiFC) analysis of self-interaction and nuclear foci localization of phosphomimic and null AHL10.

A. Quantification of relative self-interaction intensity for phosphomimic and phosphonull AHL10. Data are means ± SE, (n = 10 to 20) combined from two independent experiments. None of the phosphomimic or phosphonull constructs differed significantly from wild type in either stress or control treatments (T-test $P \leq 0.05$). Images of AHL10 self-interaction rBiFC assays are shown in SI Appendix Fig. S12.

B. Representative images of nuclear localization of AHL10 self-interaction complexes observed in rBiFC assays. Scale bars indicate 5 µm.

C. Portion of nuclei with AHL10 foci. Individual nuclei (80-130 for each construct and treatment) combined from two independent experiments were counted. Error bars indicate 95% confidence intervals and asterisks indicate significant difference compared to wild type in the same treatment (or difference of wild type stress versus control) based on Fisher's Exact test ($P \leq 0.05$).

HAI1 showed little interaction under this condition. The growth assays, gene expression analysis and localization of AHL10 complexes, demonstrated that AHL10 S314 phosphorylation was a critical determinant of AHL10 function. More broadly the data indicate roles for AHL10 and HAI1 in balancing growth versus stress and defense responses. AHL10-mediated growth suppression under moderate stress severity can be an adaptive response to reduce water use. Agronomically, such a strategy may be overly conservative and disrupting it could allow greater plant productivity in certain environments.

In some ways the effect of AHL10 to restrain growth is line with Clade A AHL (AHL15-AHL27) suppression of hypocotyl elongation (40, 43, 44). However, our results differ in that AHL10 primarily affected growth at low ψ_w and in that AHL10 is a member of the less studied Clade B AHLs (AHL1-AHL14). The only other study of AHL10 that we are aware of found AHL10 to be involved in recruitment of the heterochromatin mark Histone 3 Lysine 9 dimethylation (H3K9me2) to AT-rich transposable elements (45). We also observed mis-regulated expression of several transposons in *ahl10-1*. However, these were a minority of the differentially expressed genes, especially at low ψ_w. Whether or not histone modification or other epigenetic genetic mechanisms are involved in AHL10-mediated induction (for example *STM*, *WES1*, *DFL1*) or repression (for example *AOS, AOC1*) of gene expression is of interest for future research. The only previous report of AHL involvement in drought response found that overexpression of a rice AHL, which the authors designated as *OsAHL1*, led to enhanced survival of dehydration, salt stress or chilling stress (46). While this may at first seem inconsistent with our results, it is important to note that they measured survival of severe stress while we measured growth under moderate stress severity. It has been well noted that the mechanisms underlying survival of severe stress are distinct from those regulating growth during moderate severity drought stress (47).

Altered expression of developmental regulators *STM* and *RGF9,* auxin metabolism genes *WES1* and *DFL1* and JA metabolism genes *AOS, AOC,* as well as other AHL10-affected genes identified by RNAseq, was consistent with AHL10 effects on growth at low ψ_w. Tissue specific analysis of meristematic and growing regions could find additional AHL10-regulated genes important for growth regulation. Mine et al. (19) demonstrated that JA-induction of *HAI1* expression was involved in HAI1 suppression of MPK3 and MPK6 activation during effector triggered immunity. Our finding that HAI1-AHL10 signaling regulated JA metabolism (*AOS* and

AOC1) and JA responsive (*JR2, VSP2*) genes suggests that HAI1 also has a feedback effect on JA. This result is also consistent with other reports of cross-regulation between JA and ABA metabolism (48). In our previous characterization of HAI1, we noted that *hai1-2* had altered expression of many defense-related genes and concluded that HAI1 could be involved in trade-offs between pathogen defense and drought response (15). The current data further indicate that HAI1, AHL10 and their target genes are involved in this intersection of stress and defense signaling with growth regulation.

AT-hook proteins can associate with AT-rich sequences in matrix attachment regions (41, 42) and the C-terminal portion of AHLs is thought to mediate interaction with transcriptional regulators (40). AHL10 S314 phosphorylation was required for AHL10 complexes to form foci within the nucleoplasm. While the identity and composition of the AHL10 foci is not known, it can be hypothesized that phosphorylation-dependent interaction of AHL10 with nuclear matrix components as well as other transcriptional regulators or epigenetic factors may explain how AHL10 could act as either an inducer or suppressor of gene expression under low ψ_w. Interestingly, AHL^{S313A} had a hyperactive effect on the formation of nuclear foci and on *STM* and *WES1* expression but not *AOS1* or *AOC* (Fig. 3B). This provides one indication that different mechanisms may be involved in AHL10 up and down-regulation of gene expression. As AHL10 foci were observed in both control and low ψ_w, it is possible that the AHL10 foci are involved in repression of transposons (45), which was disrupted under both control and stress conditions in *ahl10-1*. Other, yet to be identified, phosphorylation dependent interactions of AHL10 may be involved in stress-specific effects on gene expression.

Both previous data (15) and RNAseq analysis conducted here (Dataset S6, S7) show that *HAI1* and *HAI2* are among the genes most strongly induced during low ψ_w acclimation. Along with previous physiological results (15, 19), such data indicate the prominent and distinct role that the HAI PP2Cs play in plant responses to the environment. As illustrated by our characterization of AHL10, the *hai1-2* phosphoproteomics data provide a basis to better understand the phosphatase side of the kinase-phosphatase interplay that is a central feature of stress signaling.

Materials and Methods

Phosphoproteomics analysis using ITRAQ labeling for phosphopeptide quantitation, construction of transgenic plants, low ψ_w treatment and growth assays and protein analyses were performed as previously described (11) with further details and modifications described in SI Materials and Methods. Phosphoproteomics data have been submitted to the Proteome Exchange Consortium with the data set identifier PXD004869 and RNAseq data can be accessed in the Gene Expression Onmibus (GEO) repository with accession number GSE112368.

Acknowledgements

We thank T.Z. Chang and S.-S. Huang for laboratory assistance, M.-J. Fang and J.-Y Huang for microscopy assistance and M.-Y. Lu (High Throughput Sequencing Core, Biodiversity Research Center, Academia Sinica) for RNAseq service. This work was supported by Taiwan Ministry of Science and Technology Grant 103-2314-B-001-003 (to P.E.V.).

References

1. Finkelstein R (2013) Abscisic Acid Synthesis and Response. *The Arabidopsis Book*:e0166.
2. Verslues PE (2016) ABA and cytokinins: challenge and opportunity for plant stress research. *Plant Molec Biol* 91(6):629-640.
3. Cutler SR, Rodriguez PL, Finkelstein RR, & Abrams SR (2010) Abscisic Acid: Emergence of a Core Signaling Network. *Ann Rev Plant Biol* 61:651-679.
4. Raghavendra AS, Gonugunta VK, Christmann A, & Grill E (2010) ABA perception and signalling. *Trends Plant Sci* 15(7):395-401.
5. de Zelicourt A, Colcombet J, & Hirt H (2016) The Role of MAPK Modules and ABA during Abiotic Stress Signaling. *Trends Plant Sci* 21(8):677-685.
6. Umezawa T*, et al.* (2013) Genetics and Phosphoproteomics Reveal a Protein Phosphorylation Network in the Abscisic Acid Signaling Pathway in Arabidopsis thaliana. *Sci. Signal.* 6(270):270.
7. Wang PC*, et al.* (2013) Quantitative phosphoproteomics identifies SnRK2 protein kinase substrates and reveals the effectors of abscisic acid action. *Proc Natl Acad Sci USA* 110(27):11205-11210.
8. Minkoff BB, Stecker KE, & Sussman MR (2015) Rapid Phosphoproteomic Effects of Abscisic Acid (ABA) on Wild-Type and ABA Receptor-Deficient A-thaliana Mutants. *Molec Cell Prot* 14(5):1169-1182.
9. Hoehenwarter W*, et al.* (2013) Identification of Novel in vivo MAP Kinase Substrates in Arabidopsis thaliana Through Use of Tandem Metal Oxide Affinity Chromatography. *Molec Cell Prot* 12(2):369-380.
10. Sörensson C*, et al.* (2012) Determination of primary sequence specificity of *Arabidopsis* MAPKs MPK3 and MPK6 leads to identification of new substrates. *Biochem J* 446(2):271-278.

11. Bhaskara GB, Wen TN, Nguyen TT, & Verslues PE (2017) Protein Phosphatase 2Cs and Microtubule-Associated Stress Protein 1 Control Microtubule Stability, Plant Growth, and Drought Response. *Plant Cell* 29(1):169-191.
12. Leung J*, et al.* (1994) Arabidopsis ABA response gene ABI1: features of a calcium-modulated protein phosphatase. *Science* 264(5164):1448.
13. Meyer K, Leube MP, & Grill E (1994) A protein phosphatase 2C involved in ABA signal transduction in Arabidopsis thaliana. *Science* 264(5164):1452.
14. Saez A*, et al.* (2004) Gain-of-function and loss-of-function phenotypes of the protein phosphatase 2C HAB1 reveal its role as a negative regulator of abscisic acid signalling. *Plant J* 37(3):354-369.
15. Bhaskara GB, Nguyen TT, & Verslues PE (2012) Unique Drought Resistance Functions of the Highly ABA-Induced Clade A Protein Phosphatase 2Cs. *Plant Physiol* 160(1):379-395.
16. Yoshida T*, et al.* (2006) ABA-hypersensitive germination3 encodes a protein phosphatase 2C (AtPP2CA) that strongly regulates abscisic acid signaling during germination among Arabidopsis protein phosphatase 2Cs. *Plant Physiol* 140(1):115-126.
17. Fujita Y*, et al.* (2009) Three SnRK2 Protein Kinases are the Main Positive Regulators of Abscisic Acid Signaling in Response to Water Stress in Arabidopsis. *Plant Cell Physiol* 50(12):2123-2132.
18. Wang K*, et al.* (2018) EAR1 negatively regulates ABA signaling by enhancing 2C protein phosphatase activity. *Plant Cell* 30(4): 815-834
19. Mine A*, et al.* (2017) Pathogen exploitation of an abscisic acid- and jasmonate-inducible MAPK phosphatase and its interception by Arabidopsis immunity. *Proc Natl Acad Sci USA* 114(28):7456-7461.
20. Iyer-Pascuzzi Anjali S*, et al.* (2011) Cell Identity Regulators Link Development and Stress Responses in the *Arabidopsis* Root. *Develop Cell* 21(4):770-782.
21. Bhaskara GB, Nguyen TT, Yang TH, & Verslues PE (2017) Comparative Analysis of Phosphoproteome Remodeling After Short Term Water Stress and ABA Treatments versus Longer Term Water Stress Acclimation. *Front Plant Sci* 8: 523.
22. Vlad F, Turk BE, Peynot P, Leung J, & Merlot S (2008) A versatile strategy to define the phosphorylation preferences of plant protein kinases and screen for putative substrates. *Plant J* 55(1):104-117.
23. Amanchy R*, et al.* (2007) A curated compendium of phosphorylation motifs. *Nat Biotech* 25(3):285-286.
24. Takahashi Y, Ebisu Y, & Shimazaki K (2017) Reconstitution of Abscisic Acid Signaling from the Receptor to DNA via bHLH Transcription Factors. *Plant Physiol* 174(2):815-822.
25. Merkouropoulos G, Andreasson E, Hess D, Boller T, & Peck SC (2008) An Arabidopsis protein phosphorylated in response to microbial elicitation, AtPHOS32, is a substrate of MAP kinases 3 and 6. *J Biol Chem* 283(16):10493-10499.
26. de la Fuente van Bentem S*, et al.* (2008) Site-Specific Phosphorylation Profiling of Arabidopsis Proteins by Mass Spectrometry and Peptide Chip Analysis. *J Prot Res* 7(6):2458-2470.
27. Huck NV*, et al.* (2017) Combined 15N-Labeling and TandemMOAC Quantifies Phosphorylation of MAP Kinase Substrates Downstream of MKK7 in Arabidopsis. *Front Plant Sci* 8(2050):2050.

28. Zhao SS, *et al.* (2016) CASEIN KINASE1-LIKE PROTEIN2 Regulates Actin Filament Stability and Stomatal Closure via Phosphorylation of Actin Depolymerizing Factor. *Plant Cell* 28(6):1422-1439.
29. Cui Y, *et al.* (2014) Arabidopsis *casein kinase 1-like 2* involved in abscisic acid signal transduction pathways. *J Plant Interact* 9(1):19-25.
30. Antoni R, *et al.* (2011) Selective inhibition of clade A phosphatases type 2C by PYR/PYL/RCAR abscisic acid receptors. *Plant Physiol* 158:970–980
31. Ufer G, Gertzmann A, Gasulla F, Röhrig H, & Bartels D (2017) Identification and characterization of the phosphatidic acid-binding A. thaliana phosphoprotein PLDrp1 that is regulated by PLDα1 in a stress-dependent manner. *Plant J* 92(2):276-290.
32. Barton MK & Poethig RS (1993) Formation of the shoot apical meristem in *Arabidopsis thaliana*-An analysis of development in the wild type and in the Shoot Meristemless mutant. *Development* 119(3):823-831.
33. Landrein B, *et al.* (2015) Mechanical stress contributes to the expression of the STM homeobox gene in Arabidopsis shoot meristems. *Elife* 4.
34. Park JE, *et al.* (2007) GH3-mediated auxin homeostasis links growth regulation with stress adaptation response in Arabidopsis. *J Biol Chem* 282(13):10036-10046.
35. Nakazawa M, *et al.* (2001) DFL1, an auxin-responsive GH3 gene homologue, negatively regulates shoot cell elongation and lateral root formation, and positively regulates the light response of hypocotyl length. *Plant J* 25(2):213-221.
36. Staswick PE, *et al.* (2005) Characterization of an Arabidopsis enzyme family that conjugates amino acids to indole-3-acetic acid. *Plant Cell* 17(2):616-627.
37. Matsuzaki Y, Ogawa-Ohnishi M, Mori A, & Matsubayashi Y (2010) Secreted Peptide Signals Required for Maintenance of Root Stem Cell Niche in *Arabidopsis*. *Science* 329(5995):1065-1067.
38. Laudert D & Weiler EW (1998) Allene oxide synthase: a major control point in Arabidopsis thaliana octadecanoid signalling. *Plant J* 15(5):675-684.
39. Leon-Reyes A, *et al.* (2010) Salicylate-mediated suppression of jasmonate-responsive gene expression in Arabidopsis is targeted downstream of the jasmonate biosynthesis pathway. *Planta* 232(6):1423-1432.
40. Zhao JF, Favero DS, Peng H, & Neff MM (2013) Arabidopsis thaliana AHL family modulates hypocotyl growth redundantly by interacting with each other via the PPC/DUF296 domain. *Proc Natl Acad Sci USA* 110(48):E4688-E4697.
41. Fujimoto S, *et al.* (2004) Identification of a novel plant MAR DNA binding protein localized on chromosomal surfaces. *Plant Molec Biol* 56(2):225-239.
42. Lee K & Seo PJ (2017) Coordination of matrix attachment and ATP-dependent chromatin remodeling regulate auxin biosynthesis and Arabidopsis hypocotyl elongation. *Plos One* 12(7).
43. Favero DS, *et al.* (2016) SUPPRESSOR OF PHYTOCHROME B4-#3 Represses Genes Associated with Auxin Signaling to Modulate Hypocotyl Growth. *Plant Physiol* 171(4):2701-2716.
44. Xiao CW, Chen FL, Yu XH, Lin CT, & Fu YF (2009) Over-expression of an AT-hook gene, AHL22, delays flowering and inhibits the elongation of the hypocotyl in Arabidopsis thaliana. *Plant Molec Biol* 71(1-2):39-50.

45. Jiang H, *et al.* (2017) Ectopic application of the repressive histone modification H3K9me2 establishes post-zygotic reproductive isolation in Arabidopsis thaliana. *Genes Develop* 31(12):1272-1287.
46. Zhou LG, *et al.* (2016) A novel gene OsAHL1 improves both drought avoidance and drought tolerance in rice. *Scientific Reports* 6: 30264
47. Skirycz A, *et al.* (2011) Survival and growth of Arabidopsis plants given limited water are not equal. *Nat Biotech* 29(3):212-214.
48. Wang K, *et al.* (2018) Two Abscisic Acid Responsive Plastid Lipase Genes Involved in Jasmonic Acid Biosynthesis in Arabidopsis thaliana. *Plant Cell* 30(5): 1006-1022.

Supplemental Materials
Materials and Methods
Figures S1-S13
Supplemental Datasets S1-S10